Murine norovirus inhibits B cell development in bone marrow, but does not impair antibody production in *Stat1*$^{-/-}$ mice

Daniel Eldridge

A thesis

submitted in partial fulfillment of the

requirements for the degree of

Master of Science

University of Washington

2021

Reading Committee:

Charlie C. Hsu

Brian Iritani

Jisun Paik

Program Authorized to Offer Degree:

Comparative Medicine

University of Washington

Abstract

Murine norovirus inhibits B cell development in bone marrow, but does not impair antibody production in *Stat1*$^{-/-}$ mice

Daniel Eldridge

Chair of the Supervisory Committee:

Charlie C. Hsu

Department of Comparative Medicine

Murine norovirus (MNV) is used as a model system to study human noroviruses, can infect macrophages/monocytes, neutrophils, dendritic, intestinal epithelial, T and B cells, and is highly prevalent in laboratory mice. We previously showed that MNV infection significantly reduces bone marrow B cell populations in a Stat1-dependent manner. We demonstrate here that while MNV-infected Stat1-/- mice have significant bone marrow B cell losses, expansion of splenic B cells capable of mounting an antibody response to novel antigens remains intact. We also investigated increased granulopoiesis as a mechanism of B cell loss, and we show that administration of anti-G-CSF antibody inhibits the pronounced bone marrow granulopoiesis induced by MNV infection of Stat1-/- mice, but this inhibition does not rescue bone marrow B cell losses. Therefore, these results show that MNV-infected Stat1-/- mice can still exhibit a robust humoral immune response in spite of decreased bone marrow B cells, and suggests that further investigation will be needed to identify other indirect factors or mechanisms that are

responsible for the bone marrow B cell losses seen after MNV infection. Additionally, this work adds to the knowledge about the potential physiologic effects on mice with Stat1-related disruptions in research mouse colonies that may be endemically infected with MNV.

Keywords: Norovirus, Murine Norovirus, Calicivirus, B cells, B lymphocytes, Stat1, Antibodies, Granulopoiesis

Table of Contents

Acknowledgements

I thank Kevin Mears and Olesya Pershutkina for their technical assistance in multiple aspects of this project. I also thank Dr. Charlie Hsu for his mentorship and guidance throughout the entirety of this project.

This work was supported by the Bridge Funding Program from the University of Washington.

Dedication

This work is dedicated to my wife, Betsy, and my parents, Drs. Paul and Cynthia Eldridge, who supported me endlessly across the last 11 years of my higher education pursuits. I could not have done this without them.

Introduction

Noroviruses are the most common cause of diarrhea cases across the globe, being estimated to cause over 200,000 deaths annually in developing countries, and the principal cause of foodborne disease in the United States (Hall et al., 2013; Lopman et al., 2016). Historically, study of human noroviruses was limited due to a lack of an in vitro culture systems and a lack of available animal models. However, the discovery of the first murine norovirus (MNV) reported in 2003 (Karst et al., 2003) has promoted a substantial gain in knowledge about the pathogenesis and cellular tropisms of norovirus infection. Although murine models of norovirus infection do not completely recapitulate the same clinical symptoms seen in humans after infection except in immune-compromised or neonatal animals (Kahan et al., 2011; Mumphrey et al., 2007; Roth et al., 2020), murine models are nonetheless still valuable tools to help identify pathogenic mechanisms, components of genetic susceptibility, and targets for therapies and vaccines.

Initially described to infect macrophages and dendritic cells, murine noroviruses have more recently been described to also infect neutrophils, inflammatory monocytes, T cells, and B cells, and their infection may modulate immune responses (Grau et al., 2017; Jones et al., 2014; Pearson et al., 2019; Van Winkle et al., 2018; Zhu et al., 2016). The susceptibility of myeloid cells, T cells, and B cells to infection is determined by expression of the CD300lf receptor which is necessary for viral entry (Grau et al., 2017; Haga et al., 2016; Orchard et al., 2016; Van Winkle et al., 2018).

We previously reported that MNV-4 infection causes a significant loss of developing B cells in the bone marrow which can be prevented by signal transducer and activator of transcription 1 (STAT1), an important anti-viral transcription factor (Hsu et al., 2018). We found that inhibition of B cell development by MNV-4 infection in the absence of STAT1 was likely due to a combination of direct and indirect mechanisms, rather than solely by direct infection and cell death of maturing B cells. Additionally, we reported that concurrent with these B cell losses, MNV-infected *Stat1*$^{-/-}$ mice had a profound increase in granulocytes in the bone marrow, along with significant elevations of serum granulocyte colony stimulating factor (G-CSF) (Hsu et al., 2018; Seamons et al., 2018). Therefore, in this report, we sought to determine whether the bone marrow B cell losses seen after MNV infection in *Stat1*$^{-/-}$ mice resulted in an impaired humoral immune response, and also whether the increased granulopoiesis in the bone marrow plays a role in the bone marrow B cell losses seen after MNV infection.

Given that B cells are the major antibody producing cells and can also function as antigen presenting cells, we speculated that MNV infection may have an impact on adaptive as well as innate immunity. We hypothesized that MNV infection of *Stat1*$^{-/-}$ mice would result in altered antibody production in response to novel antigenic stimulation through depletion of B cell populations and/or alteration of B cell function. Additionally, since lymphopoiesis and granulopoiesis occur in the same developmental niche in the bone marrow and exhibit a reciprocal relationship (Ueda et al., 2005), we hypothesized that prevention of granulopoiesis in the bone marrow would rescue the B cell losses observed during MNV infection. Herein, we report that despite MNV's tropism to infect B cells and despite diminished bone marrow B cell populations, MNV-infected *Stat1*$^{-/-}$ mice are capable of mounting a robust antibody response to

novel antigens comparable to the antibody responses observed in uninfected *Stat1*$^{-/-}$ mice. Furthermore, we demonstrate that MNV-induced granulopoiesis in the bone marrow of *Stat1*$^{-/-}$ mice can be inhibited by administration of anti-G-CSF antibody but this inhibition of granulopoiesis does not rescue the MNV-induced bone marrow B cell losses.

Materials and Methods

Virus:

MNV-4 was propagated in RAW 264.7 cells and plaque-assayed as previously described (Hsu et al., 2005) with the modifications of omitting HEPES and using 1% penicillin/streptomycin instead of ciprofloxacin.

Mice:

Stat1-deficient (*Stat1*$^{-/-}$) mice on a 129 background (129S6/SvEv-*Stat1*^{tm1Rds}) and wild-type (WT) 129 mice (129S6/SvEvTac) were purchased from Taconic Biosciences, Inc. (Germantown, NY). Mice were fed standard irradiated rodent chow ad libitum (Purina Lab Diet 5053, Brentwood, MO), housed in autoclaved, individually ventilated cages (Allentown, Allentown, NJ) with corncob bedding (The Andersons, Maumee, OH), and provided acidified, reverse-osmosis purified, autoclaved water in bottles. All manipulations were performed in a vertical flow animal transfer station (AniGard II, The Baker Company, Sanford, ME) disinfected with chlorine dioxide (dilution 1:18:1; Clidox S, Pharmacal Research Laboratories, Naugatuck, CT). Mice were maintained specific pathogen free via a rodent health monitoring program and were certified by the vendor to be free of specific rodent pathogens including ectoparasites, endoparasites, *Pneumocystis murina*, *Helicobacter* spp., known enteric and respiratory bacterial pathogens, and antibodies to murine norovirus, mouse hepatitis virus, Sendai virus, pneumonia virus of mice, reovirus 3, Theiler's murine encephalomyelitis virus, ectromelia virus, polyoma virus, lymphocytic choriomeningitis virus, mouse adenovirus, minute virus of mice, mouse parvovirus, mouse rotavirus, mouse cytomegalovirus, mouse thymic virus, Hantaan virus, K

virus, *Encephalitozoon cuniculi*, cilia-associated respiratory bacillus, *Mycoplasma pulmonis*, and *Clostridium piliforme*. The University of Washington's animal facilities are AAALAC-accredited and all animal studies were approved by the University of Washington's IACUC.

Experimental infections:

Mice were acclimated for at least 1 week prior to study initiation. Female, 5- to 9-week-old mice were used for experimental infections with MNV. Mice were inoculated with MNV-4 (passage 7) at ~1×10^6 PFU in 200 µL of clarified supernatants of RAW 264.7 cells per mouse by oral gavage. Clarified supernatants of uninfected RAW 264.7 cell lysates were used for control inoculations. Mice were group housed by infection status for the duration of the experiment. Mice were confirmed free of MNV prior to inoculation and MNV-4 infection status was confirmed at end of study via RT-PCR of pooled fecal samples collected from each cage. RNA extraction from feces, RT-PCR for MNV, and primers have been previously described (Hsu et al., 2015; Hsu et al., 2006).

KLH and NP-Ficoll Immunization:

Female, 5- to 9-week-old *Stat1*$^{-/-}$ and 129 wild-type mice were inoculated with MNV-4 or uninfected RAW 264.7 cell lysate by oral gavage. At 7 days post-infection (PI), mice were administered either NP-Ficoll (NPF) (50 µg per mouse, Biosearch Technologies, Beverly, MA) diluted in sterile phosphate buffered saline (PBS) by intraperitoneal injection, or Keyhole Limpet Hemocyanin (KLH) (100 µg per mouse, EMD Millipore, St. Louis, MO) suspended in TiterMax Gold Adjuvant (Sigma-Aldrich, St. Louis, MO) by subcutaneous injection. Mice were humanely euthanized via CO_2 asphyxiation at 5 weeks post-infection (4 weeks post-immunization). Two

independent experiments were performed with each experiment consisting of 4-5 mice per group.

ELISA

Whole blood at necropsy was collected into serum separator microtainers (BD Biosciences, San Jose, CA), spun down, and serum was frozen at -80°C until use. KLH- or NP-Ficoll-specific antibody levels of IgM, IgG, IgG1, IgG2a, and IgG3 in the serum was measured using AffiniPure goat anti-mouse secondary reporter antibody (Jackson ImmunoResearch, West Grove, PA) on either KLH- or NP-BSA-coated Maxisorp ELISA plates (Thermo Scientific, Wilmington, DE). Serum samples were serially diluted with PBS (1:66, 200, 600, 1800, 5400, 16200, 48600, 145800) and optical density (OD) was recorded with a Multiskan Spectrum spectrophotometer (Thermo Scientific, Wilmington, DE) at 10 minutes after ELISA substrate addition. Serum samples were run in duplicate and averaged.

G-CSF and Anti-G-CSF treatment:

Female, 5- to 9-week-old, *Stat1*$^{-/-}$ mice were administered daily intraperitoneal injections of either carrier-free recombinant mouse G-CSF protein (0.5 μg per mouse, R&D Systems, Minneapolis, MN), anti-G-CSF antibody (10 μg per mouse, monoclonal rat IgG1, clone #67604, R&D Systems, Minneapolis, MN), or control IgG isotype antibody (10 μg per mouse, monoclonal rat IgG1, clone #43414, R&D Systems, Minneapolis, MN) diluted in PBS. At the same time as intraperitoneal administrations began, mice were inoculated with MNV-4 or uninfected control lysate by oral gavage, and then humanely euthanized via CO_2 asphyxiation after 7 or 14 days of treatment. For each time point, two independent experiments were run, each

experiment with 4-5 mice per group (7 day time point) or with 6 mice per group (14 day time point).

Flow Cytometry:

Bone marrow cells harvested from the femurs and tibias of mice, and splenic cells were evaluated by flow cytometry using a BD FACSCanto II (BD Biosciences, San Jose, CA) and analyzed with FlowJo software (Tree Star, Ashland, OR). Red blood cells were lysed with ammonium-chloride-potassium lysing buffer. Bone marrow and splenic cells (1 to 2×10^6 cells) were blocked with anti-CD16/CD32 (2.4G2) antibody (Tonbo Biosciences, San Diego, CA) and stained with antibodies specific for the following cell surface markers: B220/CD45R (RA3-6B2), CD23 (B3B4), CD93 (AA4.1), CD21/CD35 (CR2/CR1) (BioLegend, San Diego, CA); CD43 (S7), Gr1-Ly6G/Ly6C (RB68C5), TCRβ (H57-597), Ly-6G (1A8), Ly-6C (AL-21), CD11b (M1/70) (BD Biosciences, San Diego, CA); IgM (Jackson ImmunoResearch, West Grove, PA). Live cells, granulocyte, or lymphocyte populations were gated based on FSC-A and SSC-A and then evaluated by cell surface markers. In the bone marrow, developing B lymphocytes were classified by phenotypic fraction as previously described (Hardy et al., 2007) and grouped: pro-B/pre-B cells (Fraction A-C', $B220^+CD43^+$), pre-B/immature B cells (Fraction D-E, $B220^{lo}CD43^-$), and long-lived mature B cells (Fraction F, $B220^{hi}CD43^-$). Granulocytes and macrophages were classified by cell surface markers as $GR\text{-}1^+CD11b^+$ and $GR\text{-}1^-CD11b^+$, respectively. Alternatively, granulocytes and macrophages were classified by $Ly6C^+Ly6G^+$ and $Ly6C^+Ly6G^-$, respectively. In the spleen, mature and transitional B cells were classified as $B220^+CD93^-$ and $B220^+CD93^+$, respectively. Mature B cells in the spleen were further classified

as follicular ($IgM^{mid}CD21^{mid}CD23^{+}$), marginal zone ($IgM^{hi}CD21^{hi}CD23^{-}$), or marginal zone precursor ($IgM^{hi}CD21^{hi}CD23^{+}$).

Statistical Analysis

Statistical analyses were performed using GraphPad Prism 9 (GraphPad Software, La Jolla, CA). An unpaired Student's t-test was used to compare 2 groups, and a one-way ANOVA with Sidak multiple comparisons test was used for greater than 2 groups. Statistical significance was defined as a *P* value of less than 0.05.

Results

MNV infection induces B cell loss in the bone marrow of *Stat1*$^{-/-}$ mice but does not impair serum antibody responses to novel antigens.

We previously reported that MNV infection resulted in a decrease in the percentage and total number of both immature and mature B cells within the bone marrow of *Stat1*$^{-/-}$ mice compared to uninfected *Stat1*$^{-/-}$ mice (Hsu et al., 2018). Since antibodies are exclusively produced by B cells during the humoral immune response, we determined whether MNV-induced B cell losses influenced the production of serum antibodies against novel antigens in vivo. Previous data showed that B cell losses could be seen as early as 7 days post-infection (PI) across all stages of developing B cells in the bone marrow (Hsu et al., 2018). Thus, WT and *Stat1*$^{-/-}$ mice were immunized with either the T-dependent (TD) antigen KLH or the T-independent (TI) antigen NPF at 7 days after MNV-4 infection to coincide the immunization with when B cell losses would start to occur. Four weeks after immunization (5 weeks PI), bone marrow was evaluated for B cell (Hardy Fractions A-F), granulocyte, and macrophage populations, while serum was evaluated for antibody isotypes and subclasses (IgM, IgG, IgG1, IgG2a, and IgG3) specific for either the KLH-TD or NPF-TI antigen.

As expected, MNV-infected *Stat1*$^{-/-}$ mice had a significant depletion in the total number of developing pro-B/pre-B cells (B220^{+}CD43^{+}, Fraction A-C'), pre-B/immature B cells (B220^{lo}CD43^{-}, Fraction D-E), and long-lived mature B cells (B220^{hi}CD43^{-}, Fraction F) in the bone marrow compared to uninfected *Stat1*$^{-/-}$ mice (Fig. 1A), whereas MNV-infected WT mice did not have significant changes in bone marrow B cell populations compared to uninfected WT

mice (Fig. 1B). Surprisingly, at 4 weeks post-immunization, all MNV-infected *Stat1*$^{-/-}$ mice were able to produce a serum antibody response close to, or in some cases, even exceeding those of uninfected *Stat1*$^{-/-}$ mice (Fig. 2), in spite of a significant loss of developing and mature B cells in the bone marrow. To compare serum antibody levels of MNV-infected vs. uninfected mice, statistical analysis (t-test) was performed at select antibody dilutions that were in the linear range of the dilution curve. In NPF-TI-immunized mice, total IgG and IgG2a were significantly increased in MNV-infected *Stat1*$^{-/-}$ mice compared with uninfected *Stat1*$^{-/-}$ mice (Fig. 2). In *Stat1*$^{-/-}$ mice immunized with either the KLH-TD or NPF-TI antigen, significantly decreased mean OD values of serum IgM were found in MNV-infected *Stat1*$^{-/-}$ mice compared to uninfected *Stat1*$^{-/-}$ mice (Fig. 2).

Since serum antibody levels were largely unchanged, and in some cases even increased in MNV-infected *Stat1*$^{-/-}$ mice despite significant decreases in developing and mature B cells in the bone marrow, we evaluated splenic B cell populations. In the spleen, follicular B cells are important for antibody production to T-dependent antigens, while marginal zone B cells are involved with antibody production to T-independent antigens (Balázs et al., 2002; Fagarasan and Honjo, 2000; Fillatreau and Gray, 2003; Martin et al., 2001; Schroeder et al., 2019). MNV-infected *Stat1*$^{-/-}$ mice immunized with either the KLH-TD or NPF-TI antigen had a significant increase in total splenic cellularity compared with uninfected *Stat1*$^{-/-}$ mice (Fig. 3). The increased splenic cellularity was largely characterized by significant increases in TCRβ^+ (T cells), B220$^+$CD93$^-$ (mature B cells), Gr1$^+$CD11b$^+$ (granulocytes), and Gr1$^-$CD11b$^+$ (macrophages) cell counts (Fig. 3). B220$^+$CD93$^+$ (transitional B cells) cell counts did not differ significantly (Fig. 4). Mature B cells were further characterized as IgM^{hi}CD21^{hi}CD23$^+$ (marginal zone precursor),

IgM^{hi}CD21^{hi}CD23^{-} (marginal zone), and IgM^{mid}CD21^{mid}CD23^{+} (follicular). After MNV-infection, marginal zone B cells in *Stat1*$^{-/-}$ mice immunized with either KLH or NPF did not significantly differ from those of similarly immunized uninfected *Stat1*$^{-/-}$ mice (Fig. 4). Interestingly, marginal zone precursor and follicular B cells were significantly increased in MNV-infected *Stat1*$^{-/-}$ mice compared to uninfected *Stat1*$^{-/-}$ mice immunized with either the KLH-TD or the NPF-TI antigen (Fig 4). These results indicate that the loss of developing and mature bone marrow B cells in MNV-infected *Stat1*$^{-/-}$ mice does not result in concurrent or proportional losses of B cell populations in the spleen, but rather some of these splenic B cell populations are in fact significantly increased.

Prevention of granulocyte proliferation during MNV infection does not rescue B cell losses in the bone marrow of MNV-infected *Stat1*$^{-/-}$ mice.

In previous studies, we observed that concurrent with the B cell losses seen in the bone morrow after MNV-infection in *Stat1*$^{-/-}$ mice, granulocytes and macrophages were significantly increased in the bone marrow (Hsu et al., 2018). We also observed that serum levels of granulocyte colony-stimulating factor (G-CSF) were increased 5.7 fold at 7 days PI and 3.9 fold at 21 days PI in MNV-4-infected *Stat1*$^{-/-}$ mice (Seamons et al., 2018). Since there is a reciprocal relationship between granulopoiesis and B lymphopoiesis in the bone marrow, and since G-CSF is a major regulator of neutrophil maturation (Rutella et al., 2005) and can suppress B lymphopoiesis in the bone marrow (Day et al., 2015; Winkler et al., 2013), we hypothesized that the loss of bone marrow B cells observed in our studies may be due to increased granulopoiesis and G-CSF induced by MNV-4 infection in *Stat1*$^{-/-}$ mice. To test this, we administered daily mouse recombinant G-CSF to uninfected *Stat1*$^{-/-}$ mice to mimic infection with MNV, or we

administered anti-G-CSF antibody to MNV-infected *Stat1*$^{-/-}$ mice in attempts to prevent bone marrow B cell losses caused by infection.

As expected, after 7 days of treatment with G-CSF, uninfected *Stat1*$^{-/-}$ mice had significant increases in bone marrow granulocyte and macrophage cell counts compared to uninfected *Stat1*$^{-/-}$ mice treated with IgG isotype control antibody (Fig. 5). Uninfected *Stat1*$^{-/-}$ mice receiving G-CSF treatment also showed a significant loss of pre-B/immature B cells (Fraction D-E) and long-lived mature B cells (Fraction F) compared with uninfected IgG isotype treated controls (Fig. 5). Pro-B/pre-B (Fraction A-C') cell counts were lower compared with uninfected isotype treated controls, but did not reach statistical significance. These results indicate that G-CSF treatment can cause granulopoiesis in the bone marrow and result in a concurrent loss of B cell populations in the bone marrow, similar to that observed after MNV-infection in *Stat1*$^{-/-}$ mice.

To determine if G-CSF plays a role in the bone marrow B cell losses seen after MNV-infection in *Stat1*$^{-/-}$ mice, anti-G-CSF antibody was administered to MNV-infected *Stat1*$^{-/-}$ mice. After 7 days of daily anti-G-CSF treatment, MNV-infected *Stat1*$^{-/-}$ mice on average had higher mean cell counts of all Hardy fractions of B cells (Fractions A-C', D-E, and F) compared to MNV-infected *Stat1*$^{-/-}$ mice treated with IgG isotype control antibody, although these differences did not reach statistical significance (Fig. 5). Anti-G-CSF treatment of MNV-infected *Stat1*$^{-/-}$ mice had lower mean cell counts of granulocytes and macrophages compared to MNV-infected IgG isotype treated controls, although only the difference in macrophage cell count reached statistical significance (Fig. 5).

Notably, in this experiment, we expected that bone marrow B cells would be significantly decreased at 7 days PI in our positive control MNV-infected *Stat1*$^{-/-}$ mice (IgG MNV+ mice) compared to our negative control uninfected *Stat1*$^{-/-}$ mice (IgG MNV- mice), similar to our previous studies. However, we found that pro-B/pre-B cells (Fraction A-C') and pre-B/immature B cells (Fraction D-E) while decreased, did not reach statistical significance likely due to minor biological variations in mouse models and/or minor variations in the kinetics of viral infection. Therefore, given that 7 days PI was the *earliest* time point that we observed a statistical differences in all bone marrow B cell populations in our previous studies (Hsu et al., 2018), we performed a second anti-G-CSF treatment experiment extending MNV-infection to 14 days, thus allowing more and sufficient time to ensure statistically significant losses of all bone marrow B cell populations in MNV-infected vs. uninfected IgG isotype treated control mice. At 14 days PI, all B cell populations were significantly decreased in MNV-infected *Stat1*$^{-/-}$ mice (IgG MNV+) compared to uninfected controls (IgG MNV-) (Fig. 6). Treatment of MNV-infected *Stat1*$^{-/-}$ mice with anti-G-CSF antibody effectively inhibited granulopoiesis in the bone marrow and also prevented increases in macrophage cell counts compared to those of MNV-infected IgG isotype controls (Fig. 6). Notably, despite the inhibition of granulopoiesis, MNV-infected mice treated with 14 days of anti-G-CSF still showed decreased bone marrow B cell counts similar to those of MNV-infected IgG isotype treated controls and were significantly lower than uninfected controls. Taken together, these data suggest that granulopoiesis induced by G-CSF alone is not responsible for the chronic impairment of B cell development observed in the bone marrow of MNV-infected *Stat1*$^{-/-}$ mice.

Discussion

In this study, we evaluated whether *Stat1*$^{-/-}$ mice would have an altered humoral immune response to novel antigens during MNV infection since MNV can infect B cells and can result in a significant depletion of both mature and immature B cells in the bone marrow (Hsu et al., 2018; Jones et al., 2014). We examined the production of serum IgM, total IgG, and three IgG subclasses in *Stat1*$^{-/-}$ mice treated with either a T-dependent or T-independent antigen in the presence or absence of MNV infection in order to assess a comprehensive antibody profile of the humoral immune response that could be impacted by direct infection of B cells or by impaired B cell development due to MNV infection. We found that MNV-infected *Stat1*$^{-/-}$ mice, in spite of a significant depletion of bone marrow B cells, are capable of mounting a robust serum antibody response to the KLH-TD or NPF-TI antigen comparable to those of uninfected mice. Given that marginal zone B cells are the primary cells responsible for the antibody response to TI antigens, and that follicular B cells are the primary cells responsible for the antibody response to TD antigens (Balázs et al., 2002; Fagarasan and Honjo, 2000; Fillatreau and Gray, 2003; Martin et al., 2001; Schroeder et al., 2019), we evaluated the splenic B cell populations of immunized mice. We found that although MNV-infected *Stat1*$^{-/-}$ mice have significantly decreased bone marrow B cell populations, they do not exhibit decreased splenic B cells numbers compared to uninfected *Stat1*$^{-/-}$ mice. Splenic B cell populations in MNV-infected *Stat1*$^{-/-}$ mice were either equivalent to those of uninfected *Stat1*$^{-/-}$ mice, or in some cases were significantly increased (e.g., marginal zone precursor and follicular B cells). Therefore, these results suggest that MNV-

infected *Stat1*$^{-/-}$ mice are still capable of mounting a robust humoral immune response to TD or TI antigens likely due to adequate or increased B cell populations in the spleen.

Interestingly, we observed that IgG2a antibody levels were increased in MNV-infected *Stat1*$^{-/-}$ mice compared to uninfected *Stat1*$^{-/-}$ mice when immunized with the NPF-TI antigen. Similarly, it has been reported that mice administered poly (I:C), a synthetic double-stranded RNA that mimics viral nucleic acids, had a greater IgG2c (expressed instead of IgG2a in certain inbred mouse strains) antibody response after immunization with NPF compared to mice administered NPF alone (Swanson et al., 2010). Although all four IgG subclasses (IgG1-4) are capable of being produced after immunization with TI antigens, the proportions of each subclass will vary as a result of the prevailing cytokine environment (Collins, 2016). After viral infection, IgG2a is the predominant antibody produced and its production is upregulated by the Th1 cytokine interferon-γ (Coutelier et al., 1987; Finkelman et al., 1988). Recently, we reported that MNV-infected *Stat1*$^{-/-}$ mice have elevated (13.9 fold increase at day 7 PI) serum interferon-γ (Seamons et al., 2018), and so this may account for the increased production of IgG2a antibody in response to immunization with a TI antigen in our current study. Although the exact biologic significance of this increase in IgG2a antibody production in MNV-infected *Stat1*$^{-/-}$ mice is not known, IgG2a has been associated with stronger FcγR-mediated activity than other antibody isotypes (Collins, 2016; Nimmerjahn and Ravetch, 2005). Specifically, IgG2a is the most efficient antibody isotype for viral clearance and for directing antibody-dependent cellular cytotoxicity (Rubtsova et al., 2013). This antibody isotype has also been shown to provide greater protection from neurologic disease induced by lactate dehydrogenase-elevating virus, lymphocytic choriomeningitis virus, or yellow fever virus (Baldridge and Buchmeier, 1992; Markine-Goriaynoff and Coutelier, 2002;

Schlesinger et al., 1993). Overall, our results suggest that while MNV infection in *Stat1*$^{-/-}$ mice results in decreased bone marrow B cells, this decrease did not result in decreased antibody production, but rather infection may have enhanced the T-independent antibody response to a novel antigen.

Also in this study, we evaluated the role of G-CSF and bone marrow granulopoiesis in the loss of bone marrow B cells in *Stat1*$^{-/-}$ mice following MNV infection. G-CSF is an important regulator for mobilization of granulocytes, hematopoietic stem cells, and other myeloid cells from the bone marrow (Basu et al., 2002; Greenbaum and Link, 2011; Rutella et al., 2005). Increased levels of G-CSF has been demonstrated in the blood and lungs of mice in response to influenza and parainfluenza infections and is critical for host survival to these infectious agents by mobilizing and recruiting activated granulocytes to promote viral clearance (Hermesh et al., 2010; Hermesh et al., 2012). Given that MNV-infected *Stat1*$^{-/-}$ mice have significant elevations in serum G-CSF and have greatly increased granulocyte populations in the bone marrow, spleen, and liver (Hsu et al., 2018; Seamons et al., 2018; Shortland et al., 2014), we hypothesized that increased granulopoiesis and G-CSF could contribute to the significant depletion of bone marrow B cells after MNV infection. In support of this, there is a reciprocal relationship between B lymphopoiesis and granulopoiesis since they both occupy a common developmental niche in the bone marrow (Ueda et al., 2004). Additionally, G-CSF has been shown to suppress B lymphopoiesis in the bone marrow via reduction of CXCL12 and IL-7 which are essential cytokines produced by stromal cells and are required for B cell development (Day et al., 2015; Winkler et al., 2013). Furthermore, G-CSF can deplete specific populations of bone marrow macrophages essential for maintaining the hematopoietic stem cell niches that give rise to

developing B cells (Winkler et al., 2010). In this study, we found that administration of exogenous G-CSF to uninfected *Stat1*$^{-/-}$ mice resulted in the significant reduction in B lymphopoiesis and concurrent increase in granulopoiesis in the bone marrow, mimicking the bone marrow changes observed after MNV-infection of *Stat1*$^{-/-}$ mice and thus suggesting a similar mechanism. To further define the role of G-CSF during MNV infection, we administered anti-G-CSF to MNV-infected *Stat1*$^{-/-}$ mice to effectively reduce granulopoiesis and bone marrow granulocyte numbers to levels similar to those of uninfected mice. Surprisingly, prevention of G-CSF-induced granulopoiesis alone was not sufficient to rescue bone marrow B cell losses after MNV-infection, as the bone marrow B cell numbers in these mice were similarly decreased compared to those of MNV-infected *Stat1*$^{-/-}$ control mice (without anti-G-CSF). Although these results suggest that G-CSF and granulopoiesis alone do not play a role in how MNV infection causes decreased bone marrow B cells in *Stat1*$^{-/-}$ mice, it is still possible that G-CSF may still be involved in a multifactorial mechanism, such as by also altering the expression of a co-factor like IL-7. We previously showed that MNV infection blunted IL-7 gene expression in MNV-infected *Stat1*$^{-/-}$ bone marrow derived macrophages (Hsu et al., 2018). We also showed that while daily administration of IL-7 to uninfected *Stat1*$^{-/-}$ mice greatly increased bone marrow B cell numbers compared to baseline levels in untreated-uninfected mice, daily administration of IL-7 to MNV-infected *Stat1*$^{-/-}$ mice only partially rescued the bone marrow B cell losses since the B cell numbers increased some but did not rise up to equivalent levels seen in uninfected IL-7 treated *Stat1*$^{-/-}$ mice (Hsu et al., 2018). Therefore, given that myeloid and lymphoid cells occupy the same developmental niche in the bone marrow, we suspect that the IL-7 treated MNV-infected *Stat1*$^{-/-}$ mice in our previous study may have been limited in their capacity to expand their bone marrow B cells to levels equivalent to those of uninfected IL-7 treated *Stat1*$^{-/-}$ mice due to the

concurrent expansion of bone marrow granulocytes caused by infection. Further investigation will be required to determine if a combination of anti-G-CSF treatment in addition to IL-7 treatment (and/or other potential co-factors such as CXCL12) would wholly rescue B cells levels to those of similarly treated, uninfected control mice.

Although our study focused on G-CSF mediated granulopoiesis and its influence on bone marrow B cells in MNV-infected *Stat1*$^{-/-}$ mice, it is still unclear why infection induces granulopoiesis and increased monocytes in these mice. A recent report by Van Winkle et al. describes recruitment of monocytes and neutrophils to sites of infection with MNV in order to promote viral persistence since these cells express the CD300lf receptor necessary for viral entry and are thus susceptible to infection (Van Winkle et al., 2018). They also reported that the cytokine IL-1α mediated this recruitment but detection of IL-1α in the serum of *Stat1*$^{-/-}$ mice at day 2 post-infection was variable and dependent on differences in the viral capsid. In our previous studies with MNV-4 in *Stat1*$^{-/-}$ mice, we were unable to detect increases in serum IL-1α at days 3, 7, or 21 after infection (Seamons et al., 2018). However, future studies may help decipher whether IL-1α may be increased locally in infected tissues, or if another mechanism is responsible for the increased granulocytes seen in the tissues of MNV-4 infected *Stat1*$^{-/-}$ mice in our studies.

Together, the studies reported here corroborate and expand upon our previous novel finding that MNV infection in the absence of *Stat1* can suppress the level of B cells in the bone marrow and induce granulopoiesis. We determined that this significant loss of developing and mature bone marrow B cells does not impair the humoral immune response to novel antigens, possibly due to

sufficient levels of B cells in peripheral sites such as the spleen. This finding is significant because it suggests that although MNV has a tropism for B cells, the functional role of antibody production is not impeded following norovirus infection even in the face of an immune-compromising condition like the absence of *Stat1* expression. We also provide evidence that the significant granulopoiesis observed during MNV infection in the absence of *Stat1* can be effectively reduced with administration of anti-G-CSF antibodies, but this reduction in granulopoiesis does not rescue the B cell losses seen in the bone marrow. Thus, our studies are important as they further add to the knowledge of norovirus pathogenesis and the potential physiologic effects on mice with *Stat1*-related disruptions in research mouse colonies that may be endemically infected with MNV.

Figures

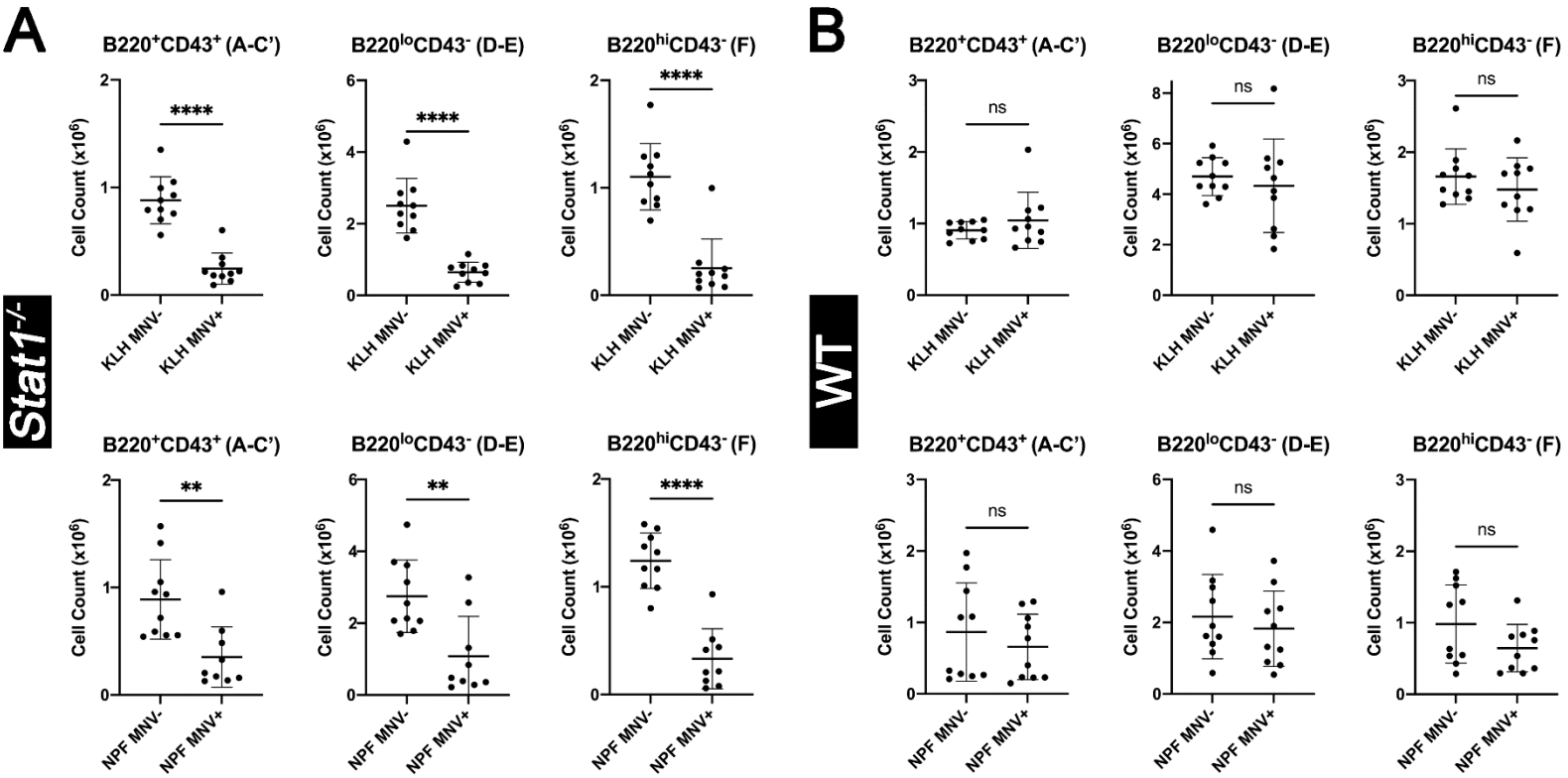

Figure 1. MNV-4 infection decreases developing bone marrow B cells in a STAT1-dependent manner. *Stat1*$^{-/-}$ mice (A) and wild-type (WT) 129 mice (B) were infected with MNV-4 or mock-inoculated, immunized 1 week post infection (PI) with KLH or NPF, and the bone marrow B cells evaluated by flow cytometry at approximately 5 weeks PI. Developing B cells were separated into pro-B/pre-B (Fraction A-C'), pre-B/immature B (Fraction D-E), and long-lived mature B (Fraction F) cells based on B220 and CD43 surface antigen staining. Data shown is combined from 2 independent experiments, each experiment with 4-5 mice per group. Bars represent mean ± SD, * = $P < 0.05$, ** = $P < 0.01$, *** = $P < 0.001$, **** = $P < 0.0001$, ns = not significant.

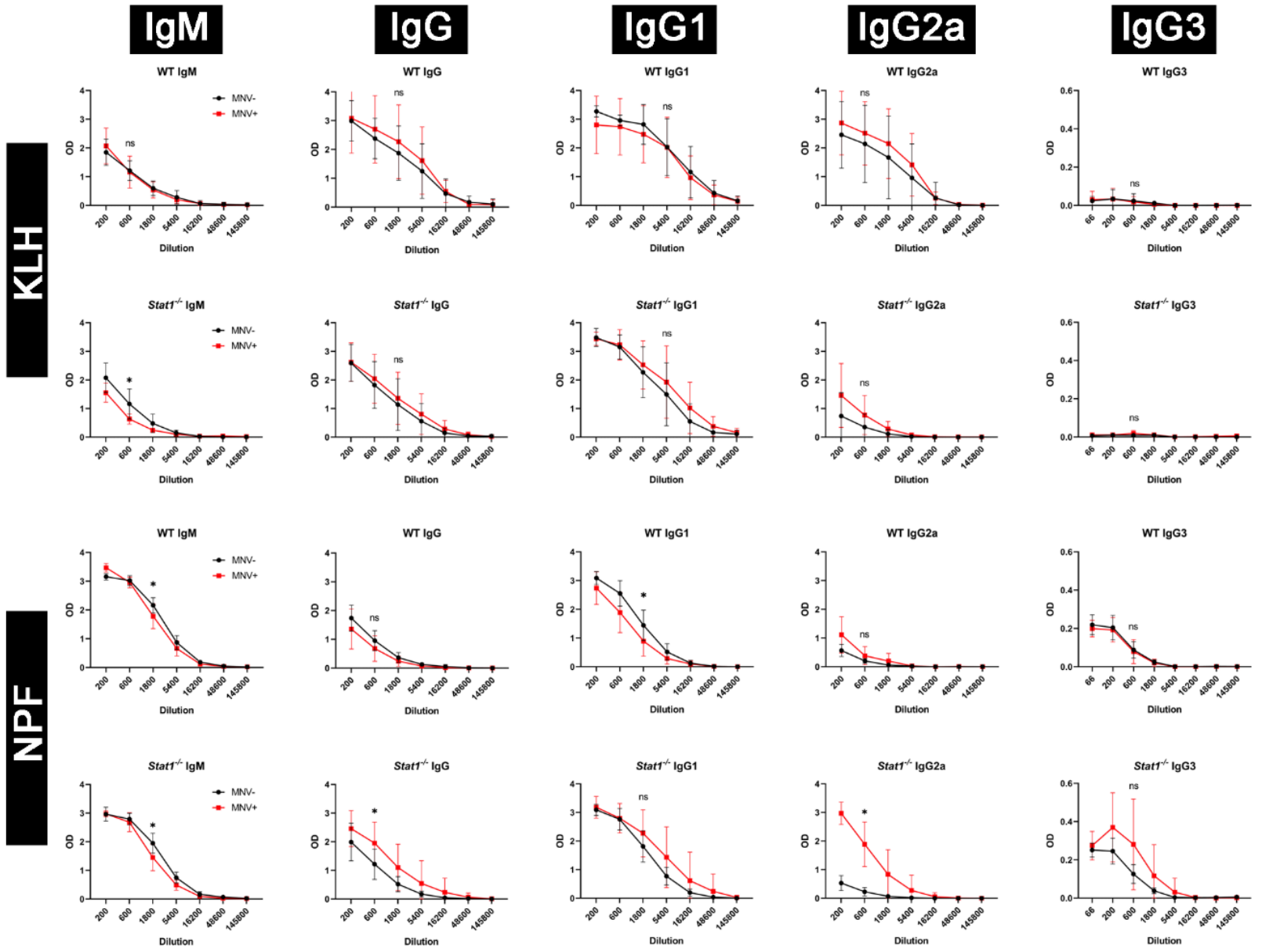

Figure 2. MNV-infected WT and *Stat1*$^{-/-}$ mice mount a robust humoral immune response to novel antigens. Wild-type (WT) 129 mice and *Stat1*$^{-/-}$ mice were infected with MNV-4 or mock-inoculated, and immunized 1 week post infection (PI) with KLH or NPF. Serum antibodies were evaluated via ELISA at 5 weeks PI. Dilution curves were generated and evaluated to ensure ELISA assays were not saturated. A dilution along a linear portion of each curve was chosen for statistical analysis. Data shown is combined from 2 independent experiments, each experiment with 4-5 mice per group. Red curves represent MNV-infected mice and black curves represent uninfected mice. Points along each curve represent mean optical density (OD) value ± SD, * = $P < 0.05$, ns = not significant.

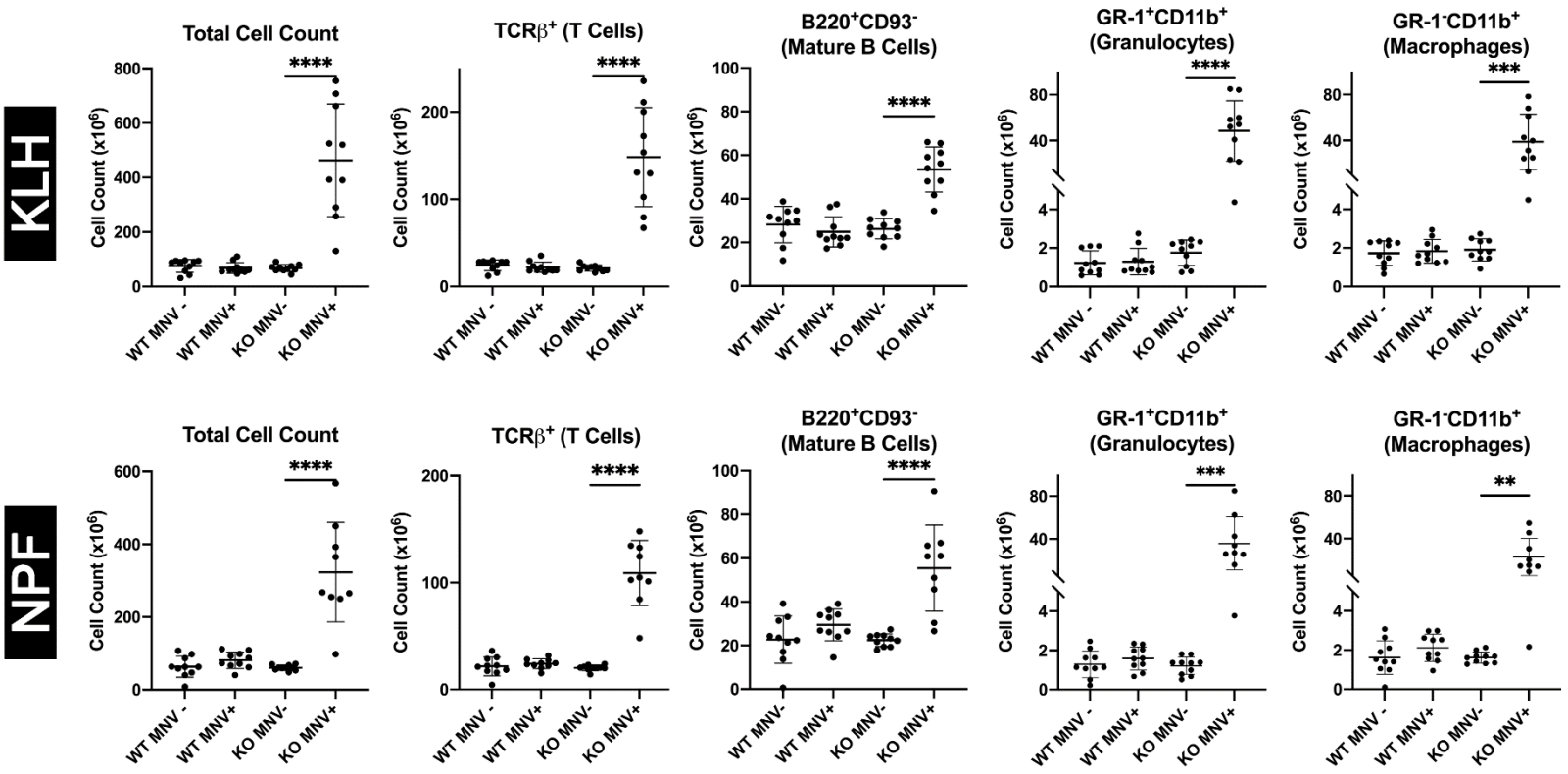

Figure 3. MNV-4 infection increases total splenic cellularity, T cells, mature B cells, granulocytes, and macrophages in a STAT1-dependent manner. Wild-type (WT) 129 mice and *Stat1*$^{-/-}$ (KO) mice were infected with MNV-4 or mock-inoculated, immunized 1 week post infection (PI) with KLH or NPF, and splenic cell populations were evaluated by flow cytometry at approximately 5 weeks PI. Cells were categorized based on cell surface antigen staining: T cells (TCRβ$^+$), mature B cells (B220$^+$CD93$^-$), granulocytes (GR-1$^+$CD11b$^+$), and macrophages (GR-1$^-$CD11b$^+$). Data shown is combined from 2 independent experiments, each experiment with 4-5 mice per group. Bars represent mean ± SD, * = $P < 0.05$, ** = $P < 0.01$, *** = $P < 0.001$, **** = $P < 0.0001$.

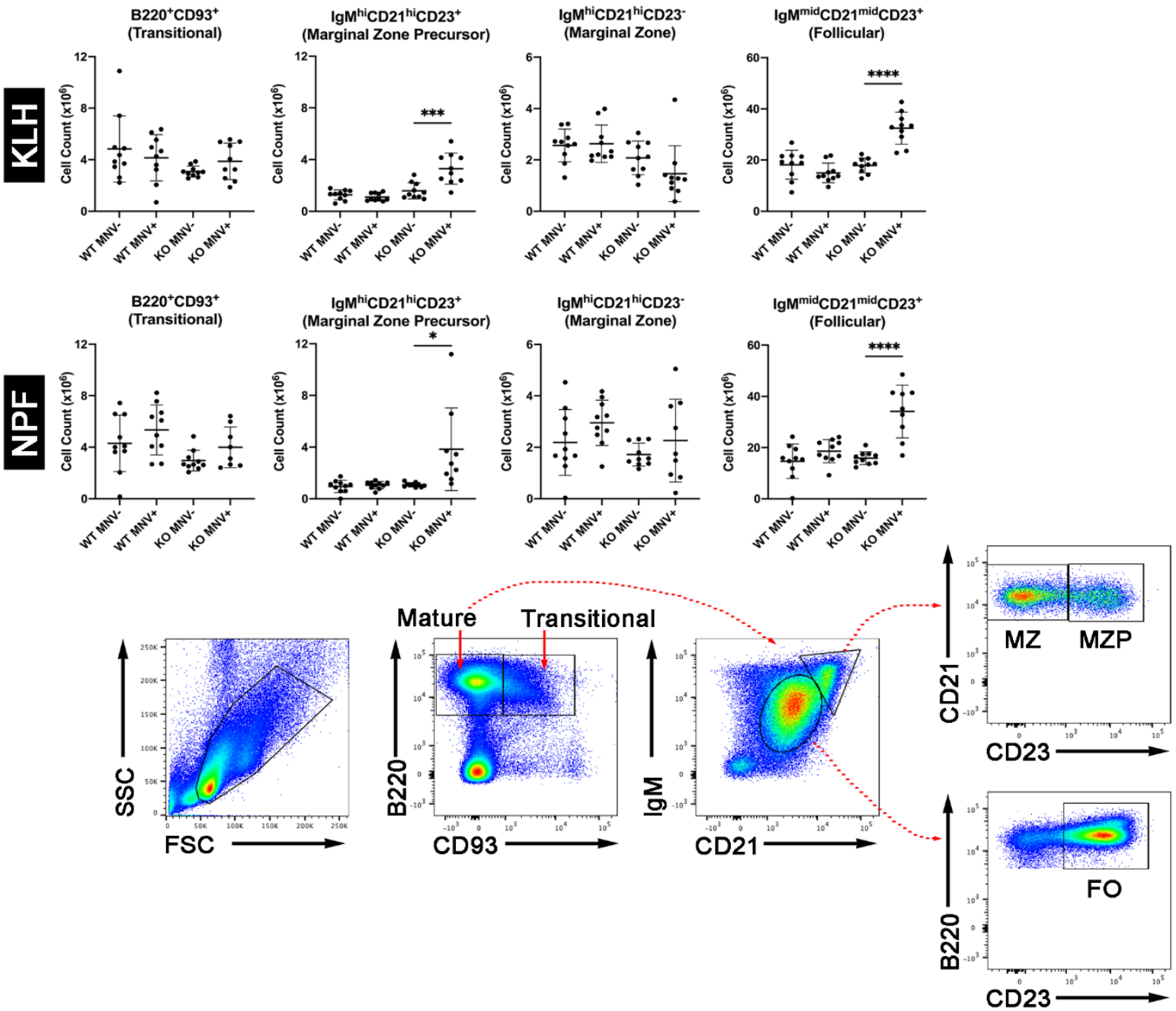

Figure 4. MNV-4 infection increases splenic mature marginal zone precursor and follicular B cell populations in a STAT1-dependent manner. Wild-type (WT) 129 mice and *Stat1*$^{-/-}$ (KO) mice were infected with MNV-4 or mock-inoculated, immunized 1 week post infection (PI) with KLH or NPF, and splenic cell populations were evaluated by flow cytometry at approximately 5 weeks PI. Mature ($B220^{+}CD93^{-}$) and transitional ($B220^{+}CD93^{+}$) B cells were separated by cell surface antigen staining. Mature ($B220^{+}CD93^{-}$) B cells were further separated into marginal zone precursors (MZP, $IgM^{hi}CD21^{hi}CD23^{+}$), marginal zone (MZ, $IgM^{hi}CD21^{hi}CD23^{-}$), and follicular (FO, $IgM^{mid}CD21^{mid}CD23^{+}$) B cells. Data shown is combined from 2 independent experiments, each experiment with 4-5 mice per group. Bars represent mean ± SD, * = $P < 0.05$, ** = $P < 0.01$, *** = $P < 0.001$, **** = $P < 0.0001$. Representative gating strategy of splenic B cell populations is shown.

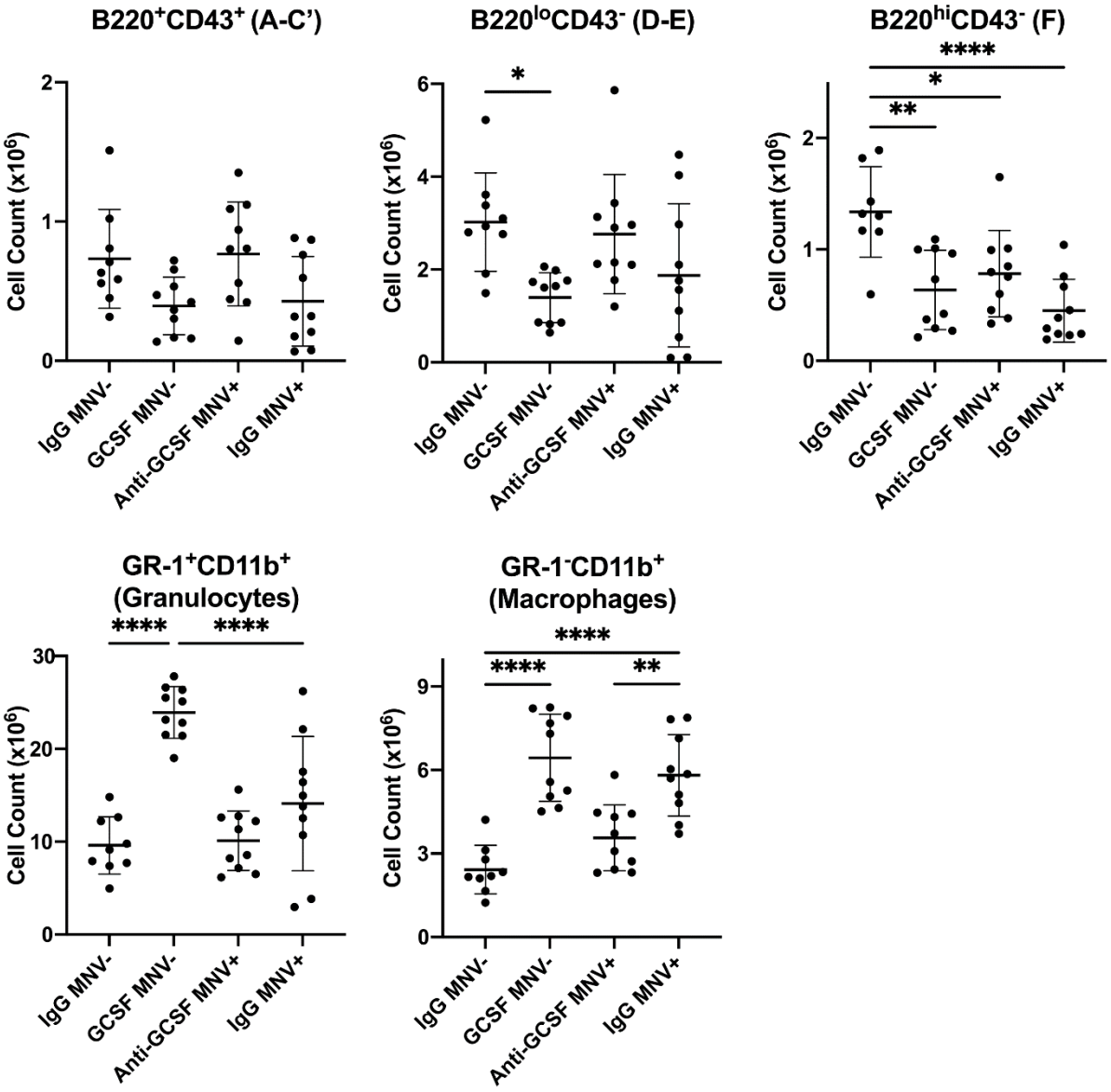

Figure 5. Exogenous G-CSF recapitulates MNV infection in *Stat1*$^{-/-}$ mice. *Stat1*$^{-/-}$ mice were infected with MNV-4 or mock-inoculated and administered daily intraperitoneal injections of recombinant G-CSF, anti-G-CSF antibody, or IgG isotype control antibody for 7 days. Bone marrow cells were evaluated by flow cytometry at 7 days post infection (PI) based on surface antigen staining: pro-B/pre-B cells (Fraction A-C'), pre-B/immature B cells (Fraction D-E), long-lived mature B cells (Fraction F), granulocytes (GR-1$^+$CD11b$^+$), and macrophages (GR-1$^-$ CD11b$^+$). Data shown is combined from 2 independent experiments, each experiment with 4-5 mice per group. Bars represent mean ± SD, * = $P < 0.05$, ** = $P < 0.01$, *** = $P < 0.001$, **** = $P < 0.0001$, ns = not significant.

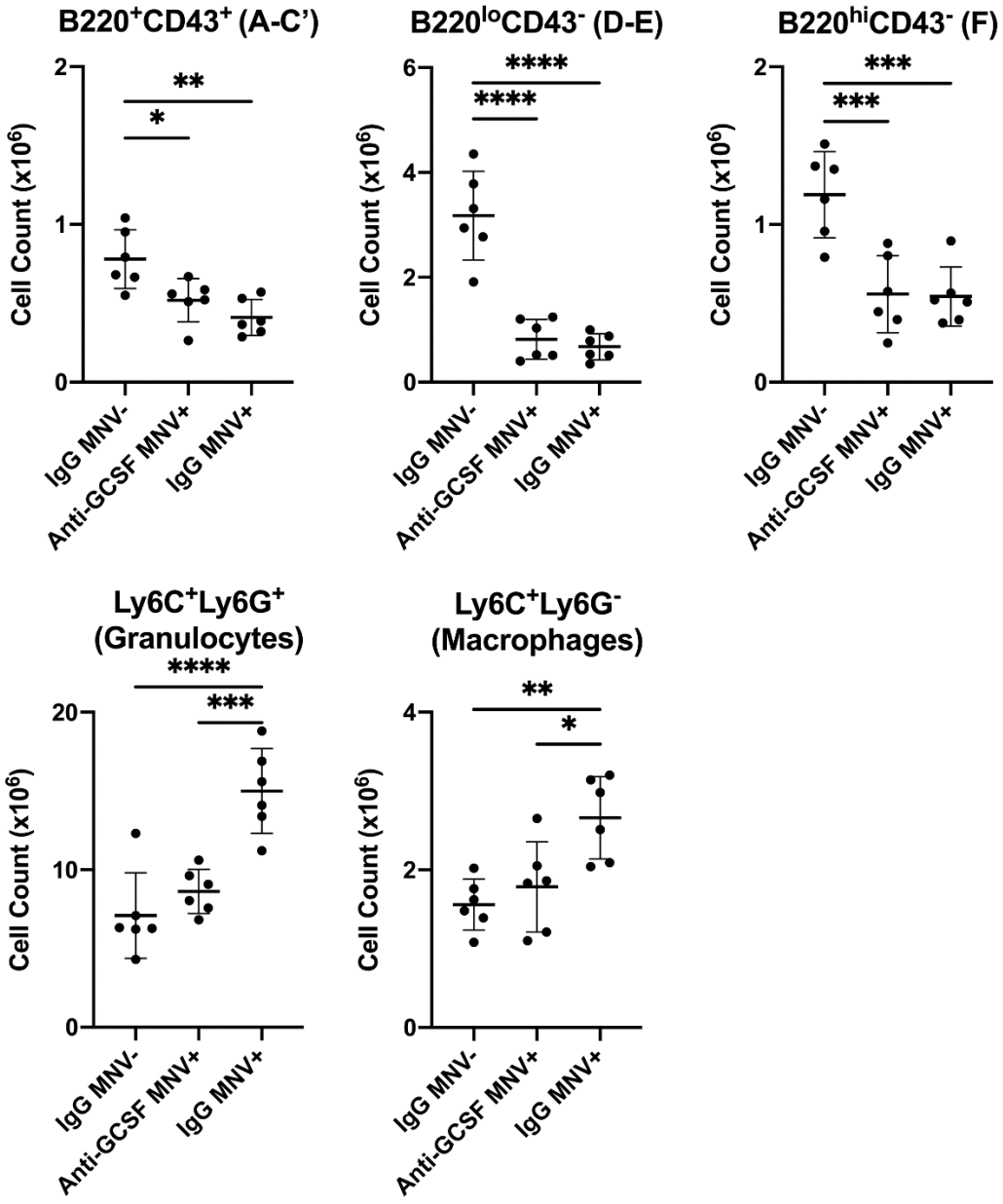

Figure 6. Prevention of granulopoiesis during MNV infection does not prevent bone marrow B cell losses in *Stat1*$^{-/-}$ mice. *Stat1*$^{-/-}$ mice were infected with MNV-4 or mock-inoculated and administered daily intraperitoneal injections anti-G-CSF antibody or IgG isotype control antibody for 14 days. Bone marrow cells were evaluated by flow cytometry at 14 days post infection (PI) based on surface antigen staining: pro-B/pre-B cells (Fraction A-C'), pre-B/immature B cells (Fraction D-E), long-lived mature B cells (Fraction F), granulocytes ($Ly6C^+Ly6G^+$), and macrophages ($Ly6C^+Ly6G^-$). N = 6 mice per group. Bars represent mean ± SD, * = $P < 0.05$, ** = $P < 0.01$, *** = $P < 0.001$, **** = $P < 0.0001$, ns = not significant.

References

Balázs, M., Martin, F., Zhou, T., Kearney, J.F., 2002. Blood Dendritic Cells Interact with Splenic Marginal Zone B Cells to Initiate T-Independent Immune Responses. Immunity 17, 341-352.

Baldridge, J.R., Buchmeier, M.J., 1992. Mechanisms of antibody-mediated protection against lymphocytic choriomeningitis virus infection: mother-to-baby transfer of humoral protection. J Virol 66, 4252-4257.

Basu, S., Hodgson, G., Katz, M., Dunn, A.R., 2002. Evaluation of role of G-CSF in the production, survival, and release of neutrophils from bone marrow into circulation. Blood 100, 854-861.

Collins, A.M., 2016. IgG subclass co-expression brings harmony to the quartet model of murine IgG function. Immunol Cell Biol 94, 949-954.

Coutelier, J.P., van der Logt, J.T., Heessen, F.W., Warnier, G., Van Snick, J., 1987. IgG2a restriction of murine antibodies elicited by viral infections. J Exp Med 165, 64-69.

Day, R.B., Bhattacharya, D., Nagasawa, T., Link, D.C., 2015. Granulocyte colony-stimulating factor reprograms bone marrow stromal cells to actively suppress B lymphopoiesis in mice. Blood 125, 3114-3117.

Fagarasan, S., Honjo, T., 2000. T-Independent immune response: new aspects of B cell biology. Science 290, 89-92.

Fillatreau, S., Gray, D., 2003. T Cell Accumulation in B Cell Follicles Is Regulated by Dendritic Cells and Is Independent of B Cell Activation. Journal of Experimental Medicine 197, 195-206.

Finkelman, F.D., Katona, I.M., Mosmann, T.R., Coffman, R.L., 1988. IFN-gamma regulates the isotypes of Ig secreted during in vivo humoral immune responses. J Immunol 140, 1022-1027.

Grau, K.R., Roth, A.N., Zhu, S., Hernandez, A., Colliou, N., Divita, B.B., Philip, D.T., Riffe, C., Giasson, B., Wallet, S.M., Mohamadzadeh, M., Karst, S.M., 2017. The major targets of acute norovirus infection are immune cells in the gut-associated lymphoid tissue. Nature Microbiology 2, 1586-1591.

Greenbaum, A.M., Link, D.C., 2011. Mechanisms of G-CSF-mediated hematopoietic stem and progenitor mobilization. Leukemia 25, 211-217.

Haga, K., Fujimoto, A., Takai-Todaka, R., Miki, M., Doan, Y.H., Murakami, K., Yokoyama, M., Murata, K., Nakanishi, A., Katayama, K., 2016. Functional receptor molecules CD300lf and CD300ld within the CD300 family enable murine noroviruses to infect cells. Proceedings of the National Academy of Sciences 113, E6248-E6255.

Hall, A.J., Lopman, B.A., Payne, D.C., Patel, M.M., Gastanaduy, P.A., Vinje, J., Parashar, U.D., 2013. Norovirus disease in the United States. Emerg Infect Dis 19, 1198-1205.

Hardy, R.R., Kincade, P.W., Dorshkind, K., 2007. The Protean Nature of Cells in the B Lymphocyte Lineage. Immunity 26, 703-714.

Hermesh, T., Moltedo, B., Moran, T.M., Lopez, C.B., 2010. Antiviral instruction of bone marrow leukocytes during respiratory viral infections. Cell Host Microbe 7, 343-353.

Hermesh, T., Moran, T.M., Jain, D., López, C.B., 2012. Granulocyte Colony-Stimulating Factor Protects Mice during Respiratory Virus Infections. PLoS ONE 7, e37334.
Hsu, C.C., Meeker, S.M., Escobar, S., Brabb, T.L., Paik, J., Park, H., Iritani, B.M., Maggio-Price, L., 2018. Murine norovirus inhibits B cell development in the bone marrow of STAT1-deficient mice. Virology 515, 123-133.
Hsu, C.C., Paik, J., Brabb, T.L., O'Brien, K.D., Kim, J., Sullivan, B.G., Hudkins, K.L., Seamons, A., Finley, J.C., Meeker, S.M., Maggio-Price, L., 2015. Murine Norovirus Infection Variably Alters Atherosclerosis in Mice Lacking Apolipoprotein E. Comp Med 65, 369-381.
Hsu, C.C., Riley, L.K., Wills, H.M., Livingston, R.S., 2006. Persistent infection with and serologic cross-reactivity of three novel murine noroviruses. Comp Med 56, 247-251.
Hsu, C.C., Wobus, C.E., Steffen, E.K., Riley, L.K., Livingston, R.S., 2005. Development of a Microsphere-Based Serologic Multiplexed Fluorescent Immunoassay and a Reverse Transcriptase PCR Assay To Detect Murine Norovirus 1 Infection in Mice. Clinical Diagnostic Laboratory Immunology 12, 1145-1151.
Jones, M.K., Watanabe, M., Zhu, S., Graves, C.L., Keyes, L.R., Grau, K.R., Gonzalez-Hernandez, M.B., Iovine, N.M., Wobus, C.E., Vinje, J., Tibbetts, S.A., Wallet, S.M., Karst, S.M., 2014. Enteric bacteria promote human and mouse norovirus infection of B cells. Science 346, 755-759.
Kahan, S.M., Liu, G., Reinhard, M.K., Hsu, C.C., Livingston, R.S., Karst, S.M., 2011. Comparative murine norovirus studies reveal a lack of correlation between intestinal virus titers and enteric pathology. Virology 421, 202-210.
Karst, S.M., Wobus, C.E., Lay, M., Davidson, J., Virgin, H.W.t., 2003. STAT1-dependent innate immunity to a Norwalk-like virus. Science 299, 1575-1578.
Lopman, B.A., Steele, D., Kirkwood, C.D., Parashar, U.D., 2016. The Vast and Varied Global Burden of Norovirus: Prospects for Prevention and Control. PLOS Medicine 13, e1001999.
Markine-Goriaynoff, D., Coutelier, J.-P., 2002. Increased efficacy of the immunoglobulin G2a subclass in antibody-mediated protection against lactate dehydrogenase-elevating virus-induced polioencephalomyelitis revealed with switch mutants. J Virol 76, 432-435.
Martin, F., Oliver, A.M., Kearney, J.F., 2001. Marginal zone and B1 B cells unite in the early response against T-independent blood-borne particulate antigens. Immunity 14, 617-629.
Mumphrey, S.M., Changotra, H., Moore, T.N., Heimann-Nichols, E.R., Wobus, C.E., Reilly, M.J., Moghadamfalahi, M., Shukla, D., Karst, S.M., 2007. Murine norovirus 1 infection is associated with histopathological changes in immunocompetent hosts, but clinical disease is prevented by STAT1-dependent interferon responses. J Virol 81, 3251-3263.
Nimmerjahn, F., Ravetch, J.V., 2005. Divergent immunoglobulin g subclass activity through selective Fc receptor binding. Science 310, 1510-1512.
Orchard, R.C., Wilen, C.B., Doench, J.G., Baldridge, M.T., McCune, B.T., Lee, Y.C.J., Lee, S., Pruett-Miller, S.M., Nelson, C.A., Fremont, D.H., Virgin, H.W., 2016. Discovery of a proteinaceous cellular receptor for a norovirus. Science 353, 933-936.
Pearson, J.A., Tai, N., Ekanayake-Alper, D.K., Peng, J., Hu, Y., Hager, K., Compton, S., Wong, F.S., Smith, P.C., Wen, L., 2019. Norovirus Changes Susceptibility to Type 1 Diabetes by Altering Intestinal Microbiota and Immune Cell Functions. Frontiers in Immunology 10.

Roth, A.N., Helm, E.W., Mirabelli, C., Kirsche, E., Smith, J.C., Eurell, L.B., Ghosh, S., Altan-Bonnet, N., Wobus, C.E., Karst, S.M., 2020. Norovirus infection causes acute self-resolving diarrhea in wild-type neonatal mice. Nat Commun 11, 2968.

Rubtsova, K., Rubtsov, A.V., van Dyk, L.F., Kappler, J.W., Marrack, P., 2013. T-box transcription factor T-bet, a key player in a unique type of B-cell activation essential for effective viral clearance. Proceedings of the National Academy of Sciences 110, E3216.

Rutella, S., Zavala, F., Danese, S., Kared, H., Leone, G., 2005. Granulocyte Colony-Stimulating Factor: A Novel Mediator of T Cell Tolerance. The Journal of Immunology 175, 7085-7091.

Schlesinger, J.J., Foltzer, M., Chapman, S., 1993. The Fc Portion of Antibody to Yellow Fever Virus NS1 Is a Determinant of Protection against YF Encephalitis in Mice. Virology 192, 132-141.

Schroeder, H.W., Radbruch, A., Berek, C., 2019. 7 - B-Cell Development and Differentiation, in: Rich, R.R., Fleisher, T.A., Shearer, W.T., Schroeder, H.W., Frew, A.J., Weyand, C.M. (Eds.), Clinical Immunology (Fifth Edition). Elsevier, London, pp. 107-118.e101.

Seamons, A., Treuting, P.M., Meeker, S., Hsu, C., Paik, J., Brabb, T., Escobar, S.S., Alexander, J.S., Ericsson, A.C., Smith, J.G., Maggio-Price, L., 2018. Obstructive Lymphangitis Precedes Colitis in Murine Norovirus-Infected Stat1-Deficient Mice. Am J Pathol 188, 1536-1554.

Shortland, A., Chettle, J., Archer, J., Wood, K., Bailey, D., Goodfellow, I., Blacklaws, B.A., Heeney, J.L., 2014. Pathology caused by persistent murine norovirus infection. J Gen Virol 95, 413-422.

Swanson, C.L., Wilson, T.J., Strauch, P., Colonna, M., Pelanda, R., Torres, R.M., 2010. Type I IFN enhances follicular B cell contribution to the T cell-independent antibody response. J Exp Med 207, 1485-1500.

Ueda, Y., Kondo, M., Kelsoe, G., 2005. Inflammation and the reciprocal production of granulocytes and lymphocytes in bone marrow. Journal of Experimental Medicine 201, 1771-1780.

Ueda, Y., Yang, K., Foster, S.J., Kondo, M., Kelsoe, G., 2004. Inflammation controls B lymphopoiesis by regulating chemokine CXCL12 expression. J Exp Med 199, 47-58.

Van Winkle, J.A., Robinson, B.A., Peters, A.M., Li, L., Nouboussi, R.V., Mack, M., Nice, T.J., 2018. Persistence of Systemic Murine Norovirus Is Maintained by Inflammatory Recruitment of Susceptible Myeloid Cells. Cell host & microbe 24, 665-676.e664.

Winkler, I.G., Bendall, L.J., Forristal, C.E., Helwani, F., Nowlan, B., Barbier, V., Shen, Y., Cisterne, A., Sedger, L.M., Levesque, J.P., 2013. B-lymphopoiesis is stopped by mobilizing doses of G-CSF and is rescued by overexpression of the anti-apoptotic protein Bcl2. Haematologica 98, 325-333.

Winkler, I.G., Sims, N.A., Pettit, A.R., Barbier, V., Nowlan, B., Helwani, F., Poulton, I.J., Van Rooijen, N., Alexander, K.A., Raggatt, L.J., Lévesque, J.-P., 2010. Bone marrow macrophages maintain hematopoietic stem cell (HSC) niches and their depletion mobilizes HSCs. Blood 116, 4815-4828.

Zhu, S., Jones, M.K., Hickman, D., Han, S., Reeves, W., Karst, S.M., 2016. Norovirus antagonism of B-cell antigen presentation results in impaired control of acute infection. Mucosal Immunol 9, 1559-1570.